Optimal Minimum Distance-Based Precoder for MIMO Spatial Multiplexing Systems

L. Collin, O. Berder, P. Rostaing, Gilles Burel

IEEE Transactions on Signal Processing, Vol. 52, No. 3, pp.617-627, March 2004
SPECIAL ISSUE ON SIGNAL PROCESSING FOR MULTIPLE-INPUT MULTIPLE-OUTPUT (MIMO) WIRELESS COMMUNICATIONS SYSTEMS

Optimal Minimum Distance Based Precoder for MIMO Spatial Multiplexing Systems

Ludovic COLLIN, *Student Member, IEEE* Olivier BERDER, *Student Member, IEEE*
Philippe ROSTAING and Gilles BUREL, *Member, IEEE*
LEST-UMR CNRS 6165, 6 Av. Le Gorgeu, BP 809, 29285 Brest Cedex, France
`Firstname.Lastname@univ-brest.fr` (fax : 33298016395)

Abstract

We describe a new precoder based on optimization of the minimum Euclidean distance $d_{\min}$ between signal points at the receiver side and for use in multiple-input multiple-output (MIMO) spatial multiplexing systems. Assuming that channel state information (CSI) can be made available at the transmitter, the three steps *noise whitening*, *channel diagonalization* and *dimension reduction*, currently used in investigations on MIMO systems, are performed. Thanks to this representation, an optimal $d_{\min}$ precoder is derived in the case of two different transmitted data streams. For QPSK modulation, a numerical approach shows that the precoder design depends on the channel characteristics. Comparisons with maximum SNR strategy and other precoders based on criteria such as water-filling (WF), minimum mean square error (MMSE) and maximization of the minimum singular value of the global channel matrix are performed to illustrate the significant bit-error-rate (BER) improvement of the proposed precoder.

Index Terms

MIMO, CSI, eigen-diagonal representation, minimum Euclidean distance, optimal linear precoder.

I. INTRODUCTION

The demand for high speed wireless links has been increasing at an amazing rate. Since a few years, multiple-input multiple output (MIMO) systems have been shown to have the potential of greatly improving the spectral efficiencies [1]. However, to fully exploit the presence of multiple antennas and achieve the promised capacity [2], appropriate precoding and/or mapping are needed.

Two main strategies in defining practical systems exist; they depend on the possibility to have channel state information (CSI) at the transmitter side. Without CSI, input symbol streams are mapped across space and time for transmit diversity and coding gain at a given data rate, which allows robust transmission even in the presence of fading [3], [4]. For duplexing schemes some information about the channel can be fedback to the transmitter. Linear precoders and decoders can then be designed through channel eigen-decomposition.

Several criteria can be used for MIMO system optimization and lead to different solutions characterized by the power allocation strategy of the transmitter. The most popular criterion is the well-known water-filling (WF) solution, which aims at maximizing the output capacity [5]. Other designs using the weighted MMSE criterion and the maximization of the minimum singular value (SV) of the channel matrix (noted $\max(\lambda_{\min})$) have been recently proposed in [6] and [7]. These optimized schemes transform the MIMO channel into parallel and independent data streams, which leads to an eigen-diagonal representation. The

solutions only differ by the power allocation strategy in this representation. The optimal power allocation strategy in the sense of the minimum bit-error-rate (BER) criterion was derived in [8]. The maximum-SNR solution [9], which consists in transmitting the whole information on the most favored subchannel, provides also very good results in term of BER (this solution is also referred to as eigenbeamforming solution in the literature).

Another interesting criterion to enhance MIMO systems performances is the minimum Euclidean distance $d_{\min}$ between signal points at the receiver side, especially when a maximum likelihood (ML) receiver is used [10]. This criterion was applied directly to design coding and modulation schemes in [11], [12]. In recent studies, it was also used to choose between transmit diversity and spatial multiplexing systems [13] or to perform a relevant antenna selection [14].

Here, we propose a precoding scheme noted $\max(d_{\min})$ by maximizing the criterion on the minimum Euclidean distance $d_{\min}$ between symbol points at the receiver side; at least for uncoded transmission, $d_{\min}$ is, indeed, directly related to symbol error rate. Coding and modulation designs are not considered here; instead, focus is only on the design of the linear precoder which is optimized for a fixed and known channel. We previously proposed in [15] a suboptimal solution of the $d_{\min}$ criterion by restricting the solution to real-valued precoders. In the present article, the results are extended to the complex case. The derivation of the $d_{\min}$ maximization design is not trivial and hence our search is restricted only to systems using two independent subchannels. This allows the use of the cos- and sin-functions system representation to obtain a closed form of the precoder. A numerical approach applied to BPSK and QPSK modulations shows that the precoder expressions always remain very simple. Even if one could see some similarity with rotated and/or scaled signal constellations [11], [16], the approach proposed in the paper is radically different because the optimized $d_{\min}$ scheme depends on the channel characteristics (*i.e.*, the channel angle defined further in section III-B). Furthermore, contrary to other precoder designs available in the literature [7] the $\max(d_{\min})$ solution is not based only on the eigen-mode power allocation. In order to evaluate the performance improvement, comparisons under an average power constraint across all transmit antennas are performed. As one may also wonder about its robustness, different scenarios are investigated, with perfect or imperfect CSI, and ML or ordered successive interference cancellation (OSIC) receivers.

The paper is organized as follows. In section II we describe the system model along with the underlying hypothesis. Section III introduces the minimum Euclidean distance criterion and the design of the optimal precoder. Section IV develops the principle of its application to spatial multiplexing systems using a BPSK modulation, whereas section V is devoted to QPSK-modulated systems. Simulation results and

comparisons with other criteria are both presented in section VI, and section VII contains our concluding remarks.

II. MIMO CHANNEL SIMPLIFIED REPRESENTATION

Let us consider a MIMO system with n_R receive and n_T transmit antennas over which we want to achieve b independent data streams. For a MIMO channel without delay spread and including a precoder matrix $\boldsymbol{F}$ and a decoder matrix $\boldsymbol{G}$, the basic system model is

$$\boldsymbol{y} = \boldsymbol{GHFs} + \boldsymbol{G\nu}, \tag{1}$$

where $\boldsymbol{H}$ is the $n_R \times n_T$ channel matrix, $\boldsymbol{F}$ is the $n_T \times b$ precoder matrix, $\boldsymbol{G}$ is the $b \times n_R$ decoder matrix, $\boldsymbol{s}$ is the $b \times 1$ transmitted vector symbol and $\boldsymbol{\nu}$ is the $n_R \times 1$ noise vector. We assume that $b \leq r = rank(\boldsymbol{H}) \leq \min(n_T, n_R)$ and [1]

$$E\{\boldsymbol{ss}^*\} = \boldsymbol{I}_b, \quad E\{\boldsymbol{\nu\nu}^*\} = \boldsymbol{R} \quad \text{and} \quad E\{\boldsymbol{s\nu}^*\} = \boldsymbol{0}. \tag{2}$$

The main objective in this section is to get a whitened noise vector and a diagonal channel matrix in order to facilitate both the system analysis and the determination of the optimal $d_{\min}$ precoder. The approach is based on the decomposition of the precoder and decoder matrices $\boldsymbol{F} = \boldsymbol{F}_v\boldsymbol{F}_D$ and $\boldsymbol{G} = \boldsymbol{G}_D\boldsymbol{G}_v$. The size of $\boldsymbol{F}_D$ and $\boldsymbol{G}_D$ is $b \times b$, whereas $\boldsymbol{F}_v$ and $\boldsymbol{G}_v$ are $n_T \times b$ and $b \times n_R$ matrices, respectively. $\boldsymbol{F}_D$ and $\boldsymbol{G}_D$ will be used to optimize $d_{\min}$. $\boldsymbol{F}_v$ and $\boldsymbol{G}_v$ are needed to obtain a full-rank diagonalized system via successive linear transformations described in Table I.

The first step is a simple noise whitening thanks to the eigen value decomposition of the noise correlation matrix $\boldsymbol{R}$. In the second step, the channel is diagonalized thanks to a singular value decomposition. In order to obtain a virtual channel matrix $\boldsymbol{H}_v$ whose size is the number of independent data streams b, the third step performs a dimensionality reduction. Finally the virtual precoder and decoder matrices are given by $\boldsymbol{F}_v = \boldsymbol{F}_1\boldsymbol{F}_2\boldsymbol{F}_3$ and $\boldsymbol{G}_v = \boldsymbol{G}_3\boldsymbol{G}_2\boldsymbol{G}_1$, respectively.

The model (1) then becomes

$$\boldsymbol{y} = \boldsymbol{G}_D\boldsymbol{H}_v\boldsymbol{F}_D\boldsymbol{s} + \boldsymbol{G}_D\boldsymbol{\nu}_v, \tag{3}$$

where $\boldsymbol{H}_v = \boldsymbol{G}_v\boldsymbol{HF}_v$ is the $b \times b$ virtual channel matrix and $\boldsymbol{\nu}_v = \boldsymbol{G}_v\nu$ is the $b \times 1$ virtual noise matrix.

Let us note p_0 the available transmission average power. We will only use virtual precoder matrices $\boldsymbol{F}_v$ with orthonormal columns, and then $\boldsymbol{F}_v^*\boldsymbol{F}_v = \boldsymbol{I}$. As a consequence, the power constraint to be fulfilled

[1] $\boldsymbol{I}_b$ denotes the $b \times b$ identity matrix and the superscript * stands for conjugate transpose.

can be expressed

$$trace\{\boldsymbol{F}\boldsymbol{F}^*\} = trace\{\boldsymbol{F}_D\boldsymbol{F}_D^*\} = p_0. \tag{4}$$

The simplified model (3) is true whatever the number of antennas and modulation. Note that the diagonal entries $\sqrt{\rho}_k$ for $k = 1, \dots b$ of $\boldsymbol{H}_v$ are sorted in decreasing order, and ρ_k is closely dependent on the SNR of the k^{th} virtual subchannel.

In the following sections, only an ML detection will be considered, and then the decoder matrix $\boldsymbol{G}_D$ will have no effect on the results. We can, therefore, assume that $\boldsymbol{G}_D = \boldsymbol{I}_b$, and then only the precoder $\boldsymbol{F}_D$ will appear in the system expressions as illustrated in Fig.1. The precoding matrix $\boldsymbol{F}_D$ remains to be determined according to the $d_{\min}$ criterion.

III. Minimum Euclidean distance precoder

A. Principle of the approach

Let us note $\mathcal{S}$ the set of all possible transmitted vectors $\boldsymbol{s}$. Thereafter, we call *received constellation* the set of all noise-free vectors $\boldsymbol{H}_v\boldsymbol{F}_D\,\boldsymbol{s}$ for $\boldsymbol{s} \in \mathcal{S}$ on the virtual receivers.

The precoder matrix $\boldsymbol{F}_D$ that maximizes the minimum Euclidean distance $d_{\min}$ of the received constellation under the power constraint $trace(\boldsymbol{F}_D\boldsymbol{F}_D^*) = p_0$ needs now to be determined. The squared $d_{\min}$ is defined by

$$d_{\min}^2 = \min_{\boldsymbol{s}_k, \boldsymbol{s}_l \in \mathcal{S},\, \boldsymbol{s}_k \neq \boldsymbol{s}_l} \|\boldsymbol{H}_v\boldsymbol{F}_D(\boldsymbol{s}_k - \boldsymbol{s}_l)\|^2. \tag{5}$$

Let us define $\breve{\boldsymbol{x}}$ a difference vector as $\breve{\boldsymbol{x}} = \boldsymbol{s}_k - \boldsymbol{s}_l$ with $k \neq l$. As many equal and collinear difference vectors exist, we introduce the reduced set $\breve{\mathcal{X}}$ of $\breve{\boldsymbol{x}}$ without all redundant difference vectors. Its use facilitates the numerical optimization of the $d_{\min}$ precoder as explained further in sections IV and IV. The $d_{\min}^2$ criterion can be expressed as

$$d_{\min}^2 = \min_{\breve{\boldsymbol{x}} \in \breve{\mathcal{X}}} \|\boldsymbol{H}_v\boldsymbol{F}_D\breve{\boldsymbol{x}}\|^2. \tag{6}$$

This criterion is particularly well adapted for the ML decision rule because the symbol error probability depends on the Euclidean distance between different received vectors [17], [18]. Indeed, as an error event comes mainly from nearest neighbors, maximization of (6) reduces directly the probability of error.

In [7] Scaglione *et al.* provided a lower bound for the minimum distance

$$d_{\min}^2 = \min_{\breve{\boldsymbol{x}} \in \breve{\mathcal{X}}} \|\boldsymbol{H}_v\boldsymbol{F}_D\breve{\boldsymbol{x}}\|^2 \geq \lambda_{\min}(SNR(\boldsymbol{F}_D)) \min_{\breve{\boldsymbol{x}} \in \breve{\mathcal{X}}} \|\breve{\boldsymbol{x}}\|^2, \tag{7}$$

where $\lambda_{\min}(SNR(\boldsymbol{F}))$ denotes the minimum eigen-value of the SNR-like matrix $SNR(\boldsymbol{F}_D)$ given by $SNR(\boldsymbol{F}_D) = \boldsymbol{H}_v\boldsymbol{F}_D\boldsymbol{F}_D^*\boldsymbol{H}_v$. They proposed a precoder $\boldsymbol{F}_D$ that maximized $\lambda_{\min}(SNR(\boldsymbol{F}_D))$

to possibly force $d_{\min}$ to higher values. This design is denoted here as the $\max(\lambda_{\min})$ solution. By definition it is equivalent to the criterion that maximizes the smallest singular value of the global channel $\boldsymbol{H}_v\boldsymbol{F}_D$ and to the *equal-error* design that ensures equal errors across subchannels for a fixed-rate system presented in [6]. It would be interesting to know whether maximization of the lower bound (7) results in performance, in term of BER, close to the $\max(d_{\min})$ criterion. Section VI will demonstrate that the proposed $\max(d_{\min})$ design actually enhances BER performance.

The determination of the precoding matrix $\boldsymbol{F}_D$ that maximizes $d_{\min}$ is difficult for two reasons: the solution depends on the symbol alphabet and the space of solutions is large. For simplification purpose the proposed technique will be derived for only $b = 2$ virtual channels by using cos- and sin- functions[2] (one should note that n_T and n_R can still be larger than 2). Thanks to this representation, the power constraint is included in the precoder and a parameterized form of $\boldsymbol{F}_D$ can be derived, which facilitates the numerical search for the optimal $d_{\min}$ precoder.

B. Parameterized form of the precoder

As only a two-dimensional virtual system is considered, the virtual channel matrix can be parameterized as follows

$$\boldsymbol{H}_v = \begin{pmatrix} \sqrt{\rho_1} & 0 \\ 0 & \sqrt{\rho_2} \end{pmatrix} = \sqrt{2\rho} \begin{pmatrix} \cos\gamma & 0 \\ 0 & \sin\gamma \end{pmatrix}, \tag{8}$$

with the channel angle γ such that $0 < \gamma \leq \pi/4$ (because $\boldsymbol{H}_v$ elements are in decreasing order) and $\rho = (\rho_1 + \rho_2)/2$.

We can perform a singular value decomposition (SVD) of the precoding matrix

$$\boldsymbol{F}_D = \boldsymbol{A}\boldsymbol{\Sigma}\boldsymbol{B}^*, \tag{9}$$

where $\boldsymbol{A}$ and $\boldsymbol{B}$ are $b \times b$ unitary matrices and $\boldsymbol{\Sigma}$ a $b \times b$ diagonal matrix with real positive values in decreasing order.

The matrix $\boldsymbol{\Sigma}$ must fulfill the power constraint across all transmit antennas (*i.e.*, $\|\boldsymbol{\Sigma}\|_F^2 = p_0$) [3]. Hence, $\boldsymbol{\Sigma}$ can be expressed as follows:

$$\boldsymbol{\Sigma} = \sqrt{p_0} \begin{pmatrix} \cos\psi & 0 \\ 0 & \sin\psi \end{pmatrix}, \tag{10}$$

with $0 \leq \psi \leq \pi/4$.

[2]These functions are, indeed, only valid for two-dimensional systems.

[3]The squared Frobenius norm of a matrix $\boldsymbol{M}$ is given by $\|\boldsymbol{M}\|_F^2 = trace(\boldsymbol{M}\boldsymbol{M}^*)$.

The singular values (SV) of $\boldsymbol{H}_v\boldsymbol{F}_D$ can be chosen from $\boldsymbol{H}_v\boldsymbol{A}\boldsymbol{\Sigma}$, because the matrix $\boldsymbol{B}^*$ has no effect on them. In Appendix I we demonstrate that the best choice for $\boldsymbol{A}$ is the identity matrix ($\boldsymbol{A} = \boldsymbol{I}_2$) because it gives the largest SV of $\boldsymbol{H}_v\boldsymbol{F}_D$ for a given angle ψ. Then, let us look for the matrices $\boldsymbol{B}$ and $\boldsymbol{\Sigma}$ that optimize $d_{\min}$. Without loss of generality, the unitary matrix $\boldsymbol{B}^*$ can be simplified as (see Appendix II)

$$\boldsymbol{B}^* = \begin{pmatrix} \cos\theta & (\sin\theta)\, e^{i\varphi} \\ -\sin\theta & (\cos\theta)\, e^{i\varphi} \end{pmatrix} = \begin{pmatrix} \cos\theta & \sin\theta \\ -\sin\theta & \cos\theta \end{pmatrix} \begin{pmatrix} 1 & 0 \\ 0 & e^{i\varphi} \end{pmatrix} = \boldsymbol{B}_\theta \boldsymbol{B}_\varphi, \tag{11}$$

with $0 \leq \theta \leq \pi/2$ and $0 \leq \varphi < 2\pi$.

The parameterized form of the precoder using cos- and sin- functions is then

$$\boldsymbol{F}_D = \sqrt{p_0} \begin{pmatrix} \cos\psi & 0 \\ 0 & \sin\psi \end{pmatrix} \begin{pmatrix} \cos\theta & \sin\theta \\ -\sin\theta & \cos\theta \end{pmatrix} \begin{pmatrix} 1 & 0 \\ 0 & e^{i\varphi} \end{pmatrix}. \tag{12}$$

Considering all the symmetries in usual constellations, it is shown in Appendix III that the influence of the angles on the Euclidean distance must be studied only for $0 \leq \varphi \leq \pi/2$ and $0 \leq \theta \leq \pi/4$.

Eq. (12) allows one to describe the effects exerted by the different angles ψ, θ and φ. ψ allocates power on each virtual receiver like the eigen-mode power allocation strategies in [6], [7]. The main difference between these schemes and (12) is the presence of the angles θ and φ that correspond to the received constellation scaling and rotation, respectively. When both are null, the matrix $\boldsymbol{F}_D$ is diagonal and equivalent to the power allocation in the eigen-mode described in [6], [7]. For instance, the $\max(\lambda_{\min})$ solution can then be found by imposing equal singular values of $\boldsymbol{H}_v\boldsymbol{F}_D$, which leads to the relation $\cos\gamma\cos\psi = \sin\gamma\sin\psi$ that must be verified by ψ.

Thanks to (12) we are now able to find the angles that give the optimal precoder according to the $d_{\min}$ criterion. A numerical approach is developed in the two following sections, devoted to the application to systems using BPSK and QPSK modulations.

IV. Simple example: optimal $d_{\min}$ precoder for a BPSK modulation

To illustrate the method let us, first, consider the simplest case: BPSK modulation. For a BPSK modulation, with $b = 2$ data streams, the symbols belong to the set $\{1, -1\}$ and the difference vectors given by the differences between the possible transmitted vectors, *i.e.* $\breve{\boldsymbol{x}} = \boldsymbol{s}_k - \boldsymbol{s}_l$ and $\boldsymbol{s}_k \neq \boldsymbol{s}_l$, are: $\left\{ \binom{0}{2}, \binom{0}{-2}, \binom{2}{0}, \binom{2}{2}, \binom{2}{-2}, \binom{-2}{0}, \binom{-2}{2}, \binom{-2}{-2} \right\}$. As some vectors are collinear, the set to be studied is reduced to: $\breve{\mathcal{X}}_{BPSK} = \left\{ \binom{0}{2}, \binom{2}{0}, \binom{2}{2}, \binom{2}{-2} \right\}$.

A numerical search over ψ, θ and φ which maximizes the smallest distance for difference vectors in $\breve{\mathcal{X}}_{BPSK}$ shows that, whatever the channel, *i.e.* whatever the channel angle γ, the precoder which maximizes $d_{\min}$ is obtained for $\psi = 0^o$, $\theta = 45^o$ and $\varphi = 90^o$, which leads to the very simple expression

$$\boldsymbol{F}_D = \boldsymbol{F}_{BPSK} = \sqrt{\frac{p_0}{2}} \begin{pmatrix} 1 & i \\ 0 & 0 \end{pmatrix}. \tag{13}$$

One should note that the second row of the precoder is null. In fact, the precoder transforms the BPSK modulation on 2 subchannels into a QPSK modulation on the most favored virtual subchannel (the first here because elements of $\boldsymbol{H}_v$ are in the decreasing order). The signal is, then, entirely transmitted on this virtual subchannel, but physically both the transmitter and the receiver do use all antennas.

The $\max(d_{\min})$ solution for the BPSK case can be seen as the $\max(SNR)$ design, which pours power only on the strongest eigenmode of the channel [19]. One should note that this $\max(SNR)$ design, also referred to as eigenbeamforming solution, is a special case of weighted MMSE design [6], obtained by choosing the weighting matrix $\boldsymbol{W} = \begin{pmatrix} 1 & 0 \\ 0 & 0 \end{pmatrix}$. A QPSK modulation used with the $\max(SNR)$ design (*i.e.*, $b = 1$ and $\boldsymbol{F}_D = \sqrt{p_0}$ in (3)) and the proposed BPSK-$\max(d_{\min})$ solution are equivalent in term of $d_{\min}$ and probability of error[4]. These two schemes have an equal and constant bit-rate.

The optimized $d_{\min}$ value is provided by the difference vectors $\binom{2}{0}$ or $\binom{0}{2}$ and its expression is

$$d_{BPSK} = \|\boldsymbol{H}_v \boldsymbol{F}_{BPSK} \binom{2}{0}\| = 2\sqrt{\rho p_0}\cos\gamma. \tag{14}$$

The distance (14) normalized by $\sqrt{2\rho p_0}$ and the corresponding BER performances are plotted in Fig. 2 and in Fig. 7, respectively.

V. Optimal $d_{\min}$ precoder for a QPSK modulation

In order to respect the assumption $E\{\boldsymbol{s}\boldsymbol{s}^*\} = \boldsymbol{I}_b$, the symbols belong to the following set: $\left\{\frac{1}{\sqrt{2}}(1+i), \frac{1}{\sqrt{2}}(1-i), \frac{1}{\sqrt{2}}(-1+i), \frac{1}{\sqrt{2}}(-1-i)\right\}$. As in the BPSK case, the set of received difference vectors $\breve{\boldsymbol{x}}$ can be reduced [5] to a set denoted $\breve{\mathcal{X}}_{QPSK}$ of only 14 elements $\{\breve{\boldsymbol{a}}, \breve{\boldsymbol{b}}, \ldots, \breve{\boldsymbol{n}}\}$.

A numerical search over ψ, θ and φ which maximize $d_{\min}$ for each channel angle γ shows that the precoder can have two different expressions. If γ stays under a threshold γ_0, then the precoder uses only the most favored subchannel as in the BPSK case and it will be noted $\boldsymbol{F}_{r1}$. On the other hand, if $\gamma \geq \gamma_0$, the precoder leads to an octagonal received constellation on both receivers, and it will be noted $\boldsymbol{F}_{octa}$.

[4]The received virtual constellations of these two schemes are strictly identical.

[5]For a QPSK modulation with $b = 2$ data streams, the set of all possible difference vectors has $16 \times 15 = 240$ elements.

The exact value of the threshold is computed on considering that both expressions provide the same $d_{\min}$ for γ_0.

A. Precoder $\boldsymbol{F}_{r1}$

For any channel parameter $\gamma \leq \gamma_0$, the numerical maximization of $d_{\min}$ gives the angles $\psi = 0$, $\varphi = 15^o$ and $\theta \simeq 27.37^o$. The exact values of φ and θ are analytically given in Appendix IV and are used in (12) to express our precoder

$$\boldsymbol{F}_{r1} = \sqrt{p_0} \begin{pmatrix} \sqrt{\frac{3+\sqrt{3}}{6}} & \sqrt{\frac{3-\sqrt{3}}{6}} e^{i\frac{\pi}{12}} \\ 0 & 0 \end{pmatrix}. \tag{15}$$

Fig. 3 illustrates the received constellation obtained with $\boldsymbol{F}_{r1}$. Only the first virtual receiver is considered because the second subchannel is not used by $\boldsymbol{F}_{r1}$. The received constellation looks like a 15^o rotated 16-QAM constellation. This solution is close to the $\max(SNR)$ design used with a 16-QAM modulation, but provides a slightly larger $d_{\min}$.

The optimized $d_{\min}$ is always obtained from the difference vector $\binom{0}{-\sqrt{2}}$. As a consequence, we immediately get the optimal $d_{\min}$ for the precoder $\boldsymbol{F}_{r1}$

$$d_{r1} = \|\boldsymbol{H}_v \boldsymbol{F}_{r1} \begin{pmatrix} 0 \\ -\sqrt{2} \end{pmatrix}\| = \sqrt{2\rho p_0} \sqrt{\frac{\sqrt{3}-1}{\sqrt{3}}} \cos\gamma. \tag{16}$$

The distance (16) normalized by $\sqrt{2\rho p_0}$ is plotted in Fig. 6 and the performance of this precoder is discussed in section VI.

B. Octagonal precoder $\boldsymbol{F}_{octa}$

For any $\gamma \geq \gamma_0$, the angles φ and θ are fixed, as for precoders $\boldsymbol{F}_{BPSK}$ and $\boldsymbol{F}_{r1}$. On the other hand ψ depends on γ, which allows power allocation on the two virtual subchannels. The precoder turns each quarter (*e.g.*, points A,E,M and I in Fig. 5) of the received constellation by $\varphi = 45^o$ and mixes the two components ($\theta = 45^o$). This clever solution found by the precoder is illustrated for both virtual subchannels in Fig. 5, where the vectors on the received constellation are labeled from A to P. One should note that whenever two received vectors are close on one virtual subchannel, *e.g.* G and L on the first virtual subchannel, they are distant on the second one. As the received constellation looks like two concentric octagons, the precoder is denoted $\boldsymbol{F}_{octa}$ and expressed as a function of ψ

$$\boldsymbol{F}_{octa} = \sqrt{p_0} \begin{pmatrix} \cos\psi & 0 \\ 0 & \sin\psi \end{pmatrix} \frac{1}{2} \begin{pmatrix} \sqrt{2} & 1+i \\ -\sqrt{2} & 1+i \end{pmatrix}. \tag{17}$$

The global channel expression is then

$$\boldsymbol{H}_v\boldsymbol{F}_{octa} = \sqrt{2\rho p_0}\begin{pmatrix}\cos\gamma\cos\psi & 0\\ 0 & \sin\gamma\sin\psi\end{pmatrix}\frac{1}{2}\begin{pmatrix}\sqrt{2} & 1+i\\ -\sqrt{2} & 1+i\end{pmatrix}. \tag{18}$$

Fig. 4 plots the norm of the 14 received difference vectors with respect to ψ for a given channel (here $\gamma = 30^o$). The value of ψ that maximizes the minimum Euclidean distance of the precoder is at the intersection of the curves relative to $\breve{\boldsymbol{a}} = \binom{\sqrt{2}}{0}$ and $\breve{\boldsymbol{b}} = \binom{\sqrt{2}}{-\sqrt{2}}$. These results can be observed for any γ in $]0, \pi/4]$.

If we denote $d_{\breve{a}}$ and $d_{\breve{b}}$ the distances related to difference vectors $\breve{\boldsymbol{a}}$ and $\breve{\boldsymbol{b}}$ respectively, the optimal precoder is obtained when $d_{\breve{a}} = d_{\breve{b}}$. The use of the global channel expression (18) leads to

$$\begin{aligned} d_{\breve{a}} &= \|\boldsymbol{H}_v\boldsymbol{F}_{octa}\breve{\boldsymbol{a}}\| = \sqrt{2\rho p_0}\sqrt{\cos^2\gamma\cos^2\psi + \sin^2\gamma\sin^2\psi}\\ d_{\breve{b}} &= \|\boldsymbol{H}_v\boldsymbol{F}_{octa}\breve{\boldsymbol{b}}\| = \sqrt{2\rho p_0}\sqrt{(2-\sqrt{2})\cos^2\gamma\cos^2\psi + (2+\sqrt{2})\sin^2\gamma\sin^2\psi}. \end{aligned} \tag{19}$$

By considering $d_{\breve{a}} = d_{\breve{b}}$, we get ψ with respect to γ:

$$\tan\psi = \frac{\sqrt{2}-1}{\tan\gamma}. \tag{20}$$

One should note that for $\gamma = \pi/6$, the value $\psi = 35.6^o$ given by (20) can be found on Fig. 4.

The precoder $\boldsymbol{F}_{octa}$ is then computed by substituting (20) in (17), which finally gives the optimal $d_{\min}$ ruled only by the channel angle γ

$$d_{octa} = \sqrt{2\rho p_0}\cos\gamma\ \cos\psi\ \sqrt{4-2\sqrt{2}} = \sqrt{2\rho p_0}\sqrt{\frac{(4-2\sqrt{2})\cos^2\gamma\sin^2\gamma}{1+(2-2\sqrt{2})\cos^2\gamma}}. \tag{21}$$

This normalized distance (*i.e.*, $d_{octa}/\sqrt{2\rho p_0}$) is plotted in Fig. 6 and the performance of this precoder is discussed in section VI.

C. Channel optimal threshold γ_0

The optimal distances previously obtained are only governed by the channel parameter γ. To choose between $\boldsymbol{F}_{r1}$ and $\boldsymbol{F}_{octa}$ and get the corresponding threshold, we have to look for the value γ_0 such that $d_{r1} = d_{octa}$ (cf Fig. 6). From (16) and (21) we get

$$\cos\psi = \sqrt{\frac{\sqrt{3}-1}{\sqrt{3}(4-2\sqrt{2})}}, \tag{22}$$

and (20) leads to

$$\tan^2\gamma_0 = \frac{3\sqrt{3}-2\sqrt{6}+2\sqrt{2}-3}{3\sqrt{3}-2\sqrt{6}+1} \simeq 0.0968 \qquad \text{and} \qquad \gamma_0 \simeq 17.28^o. \tag{23}$$

One should note that $\tan^2\gamma$ corresponds to a ratio between the virtual subchannels SNRs. In fact from (8) we get $\frac{1}{\tan^2\gamma} = \frac{\cos^2\gamma}{\sin^2\gamma} = \frac{\rho_1}{\rho_2}$. This SNRs ratio determines the optimal $d_{\min}$ precoder: $\boldsymbol{F}_{octa}$ for $\frac{\rho_1}{\rho 2} \leq \frac{1}{\tan^2\gamma_0} \simeq 10.33$ and $\boldsymbol{F}_{r1}$ for $\frac{\rho_1}{\rho_2} \geq 10.33$.

In the QPSK case, the $\max(d_{\min})$ solution can be seen as power and bit loading at constant power and constant bit-rate, since $\boldsymbol{F}_{r1}$ and $\boldsymbol{F}_{octa}$ precoders are selected according to the channel angle γ_0. When the $\boldsymbol{F}_{r1}$ precoder is chosen, 4-bit information is transmitted over the strongest eigenmode like the $\max(SNR)$ design and when the $\boldsymbol{F}_{octa}$ precoder is chosen, 2-bit information is transmitted on each virtual subchannel. Furthermore, the $\max(d_{min})$ solution brings the possibility to scale and rotate the received constellation.

VI. Simulation results

Through Monte-Carlo simulations this section illustrates how the max($d_{\min}$) precoder improves BER performances of MIMO systems. We consider a MIMO channel with $n_T = 3$ transmit antennas and $n_R = 2$ receive antennas over which we send $b = 2$ independent data streams. Entries of the channel matrix $\boldsymbol{H}$ are considered to be i.i.d. complex Gaussian random variables with mean zero and variance equal to one, and are chosen every block of 100 transmitted symbol vectors. The noise vector elements are zero-mean i.i.d. complex Gaussian with variance σ^2. As the received power depends on the precoder coefficients, the SNR is defined as the ratio of the total transmitted power to the total received noise power and is given by $SNR = p_0/(n_R\sigma^2)$. For each SNR, 20 000 random $\boldsymbol{H}$ are generated; the precoders are optimized for each of them, given perfect or imperfect CSI at both the transmitter and the receiver. An ML receiver is assumed, and five precoders are compared for BPSK and QPSK modulations[6]: $\max(d_{\min})$, $\max(SNR)$, MMSE [6], WF [5] and $\max(\lambda_{\min})$.

In Figs. 2 and 6 are plotted the normalized distance (*i.e.*, $d_{\min}/\sqrt{2\rho p_0}$) for each precoder, in the case of BPSK and QPSK modulations, respectively. One should note that in the MMSE and WF cases, $\sqrt{2\rho p_0}$ is chosen large enough such that the precoders always allocate power to the two eigenmodes. As discussed in section IV the optimized $d_{\min}$ for the BPSK is equivalent to the $\max(SNR)$ design with a $QPSK$ modulation, so the latter is not plotted in Fig.2. The $\max(\lambda_{\min})$ solution is better than the MMSE and WF solution in term of $d_{\min}$, but is really outperformed by the new $d_{\min}$ precoder. We can expect then a large performance improvement in term of BER in comparison to the diagonal precoders because the

[6]In the case of the $\max(SNR)$ design, the constellation size is squared since it uses only $b = 1$ data stream in order to perform comparisons at constant bit rate.

minimum distance is improved significantly. In Fig. 6, we observe that the difference between F_{r1} and $\max(SNR)$ remains constant for every channel angle γ. The gain for F_{r1} comes from the rotation of 15^o of a 16-QAM which slightly improves the $d_{\min}$.

Figs. 7 and 8 plot BER with respect to the SNR for BPSK and QPSK modulations. These results clearly demonstrate that the $\max(d_{\min})$ criterion is particularly suited for BER minimization when a ML receiver is used since it outperforms the diagonal precoders. Furthermore, we observe in Fig. 8 at high SNR a performance improvement of about $1\,dB$ in comparison to the $\max(SNR)$.

In the QPSK modulation case, the BER improvement depends on the channel characteristics. To differentiate the performance of $\boldsymbol{F}_{r1}$ and $\boldsymbol{F}_{octa}$, we extract from Fig. 8 the cases when $\frac{\rho_1}{\rho_2} \leq 10.33$ ($\boldsymbol{F}_{octa}$) and $\frac{\rho_1}{\rho_2} \geq 10.33$ ($\boldsymbol{F}_{r1}$). Figs. 9 and 10 plot the corresponding BER curves. As expected when looking at the normalized $d_{\min}$ in (6), the improvement is more significant when using the $\boldsymbol{F}_{r1}$ precoder in comparison with diagonal precoders. One should remain that $\boldsymbol{F}_{r1}$ is automatically selected when there is a large dispersion of the subchannels SNRs ρ_1 and ρ_2 (this case represents about 17.4% of our channel realizations). However, we observe a light superiority of $\max(SNR)$ (Fig. 10) in spite of its inferiority in term of d_{min}. This can be explained by two reasons: *i)* for the $\max(d_{min})$ precoder, the bit coding on the received constellation is not optimized *ii)* the number of neighbors is statistically more important due to the maximization of $d_{\min}$, *e.g.* the point 'J' in Fig. 3 has 5 neighbors. As a consequence, the performance improvement of the $\max(d_{min})$ in comparison to the $\max(SNR)$ comes from F_{octa}, as illustrated on Fig. 9.

Whenever an ML receiver is used with $\max(\lambda_{\min})$, MMSE or WF precoding, this receiver can be considered as linear since the virtual subchannels appear parallel and independent. In this case, the ML receiver simply inverse the virtual subchannels. Contrary to these schemes, the $d_{\min}$-based precoder is not diagonal and is not subject to a diversity loss, which results in the slopes difference visible on Fig. 8. One may wonder about the $\max(d_{\min})$ precoder performances with another receiver algorithm. Part of response is given by Fig. 11 which plots the BER when an OSIC receiver described in [20] is used. Even if there is a loss of about $2\,dB$ in comparison to the optimal ML receiver, these BER curves confirm the assets of the $\max(d_{\min})$ precoder.

In Fig.12 we investigate the impact of imperfect channel knowledge at both transmitter and receiver on the BER performance. In general, the estimated channel matrix $\boldsymbol{H}_{est}$ is modeled as $\boldsymbol{H}_{est} = \boldsymbol{H} + \boldsymbol{H}_{err}$ where $\boldsymbol{H}_{err}$ represents the channel estimation error. A more complete description of $\boldsymbol{H}_{est}$ can be found in [21] for two different methods of channel estimation. It is assumed here that entries of $\boldsymbol{H}_{err}$, independent of $\boldsymbol{H}$, are complex Gaussian i.i.d random variables with mean zero and variance σ^2_{err}. Higher the SNR

is, smaller σ_{err}^2 is; in our simulations we set $\sigma_{err}^2 = \beta\sigma^2$ with $\beta = 0.25$. The performance of all schemes decreases (of about 1 dB at high SNR), but the gap between the $\max(d_{\min})$ and the $\max(SNR)$ remains unchanged.

VII. Conclusion

We introduced a new two-dimensional precoder for MIMO transmission, which is based on the maximization of the minimum Euclidean distance on the received constellation for a given transmit average power constraint. Given perfect CSI at the transmitter, we obtained in a first step a fast and simple diagonal representation apart from channel matrices successive decompositions. Thanks to this representation, the $\max(d_{\min})$ precoder was derived in the case of two-dimensional subchannels. One should underline that the number of antennas at the transmitter and receiver is not restricted to 2 and can by chosen such that $2 \leq \min(n_T, n_R)$. With BPSK modulation the optimal $d_{\min}$ precoder uses only the most favored virtual subchannel. It is worth noting that even if the worst virtual channel is dropped both the transmitter and receiver use physically the whole set of antennas. The BPSK-$\max(d_{\min})$ design is equivalent in term of $d_{\min}$ and BER to the $\max(SNR)$ design with a QPSK modulation. In the QPSK modulation case, we showed that the precoder design is governed by the channel angle, which leads to two distinct cases separated by a precise threshold channel angle. With a large dispersion between the subchannels SNRs, the design is the same as the one in the BPSK case (only one virtual subchannel in use); otherwise the precoder produces an octagonal received constellation on each virtual subchannel. Comparisons to diagonal precoders, based on WF, MMSE or $\max(\lambda_{\min})$ criteria were performed to illustrate the significant improvement in term of BER. The performance improvement of the QPSK-$\max(d_{\min})$ design is about $1\,dB$ in comparison to the $\max(SNR)$ at equal and constant bit-rate. Finally, the robustness of the $\max(d_{\min})$ precoder is confirmed by simulations with imperfect CSI and with an OSIC receiver. It would be interesting to generalize these novel results to the case of $b > 2$, but a new formalism would be needed. On the other hand, the method developed in this paper can be directly extended to higher order modulations only by performing a new numerical search with adapted difference vectors.

Acknowledgment

The authors would like to thank the reviewers for their very useful and interesting comments and remarks which have contributed significantly to improve the content of the paper.

APPENDIX I
PROOF OF $\boldsymbol{A} = \boldsymbol{I}_2$

Let us consider the general form of the unitary matrix $\boldsymbol{A}$ defined by

$$\boldsymbol{A} = \begin{pmatrix} (\cos\alpha)\, e^{i\alpha_1} & (\sin\alpha)\, e^{i\alpha_3} \\ -(\sin\alpha)\, e^{i\alpha_2} & (\cos\alpha)\, e^{i\alpha_4} \end{pmatrix} \tag{24}$$

with the constraint

$$(\alpha_1 + \alpha_4) = (\alpha_2 + \alpha_3) \qquad \mod\ 2\pi. \tag{25}$$

The angle α must be in the interval $0 \leq \alpha < \pi/2$ (such that the expressions before the exponentials are positive and correspond to the modules). It can be verified that the two columns of $\boldsymbol{A}$ are orthonormal.

Our objective in this appendix is to find the matrix $\boldsymbol{A}$ which gives the highest singular values of $\boldsymbol{H}_v\boldsymbol{F}_D$ for a given angle ψ defined in (10) . We first show that $\boldsymbol{A}$ can be a real matrix, then that the highest SV are given by $\boldsymbol{A} = \boldsymbol{I}_2$.

One should remind that the SV are real and positive (or null) and that the determinant of a unitary matrix has a module equal to 1. Let us note $\boldsymbol{U}\boldsymbol{\Lambda}\boldsymbol{V}^*$ the SVD of $\boldsymbol{H}_v\boldsymbol{A}\boldsymbol{\Sigma}$ and λ_k the diagonal elements of $\boldsymbol{\Lambda}$ (*i.e.*, the SV of $\boldsymbol{H}_v\boldsymbol{A}\boldsymbol{\Sigma}$). The product of the SV does not depend on $\boldsymbol{A}$. Indeed, we can write

$$\begin{aligned} \lambda_1\lambda_2 &= |\det(\boldsymbol{\Lambda})| = |\det(\boldsymbol{U}\boldsymbol{\Lambda}\boldsymbol{V}^*)| = |\det(\boldsymbol{H}_v\boldsymbol{A}\boldsymbol{\Sigma})| \\ &= |\sqrt{\rho_1\rho_2}p_0\cos\psi\sin\psi\det(\boldsymbol{A})| = \sqrt{\rho_1\rho_2}p_0\cos\psi\sin\psi. \end{aligned} \tag{26}$$

Furthermore, as far as the sum of the square SV is concerned, we have

$$\lambda_1^2 + \lambda_2^2 = trace\left(\boldsymbol{\Lambda}^{\boldsymbol{2}}\right) = trace\left(\boldsymbol{U}\boldsymbol{\Lambda}\boldsymbol{V}^*\boldsymbol{V}\boldsymbol{\Lambda}\boldsymbol{U}^*\right) = \|\boldsymbol{U}\boldsymbol{\Lambda}\boldsymbol{V}^*\|_F^2 = \|\boldsymbol{H}_v\boldsymbol{A}\boldsymbol{\Sigma}\|_F^2. \tag{27}$$

Hence, the phases of the elements of $\boldsymbol{A}$ have no influence on $\lambda_1^2 + \lambda_2^2$.

Finally, we can conclude that the SV do not depend on the phases of the elements of $\boldsymbol{A}$. Then we can consider real matrices $\boldsymbol{A}$ only, whose general form is

$$\boldsymbol{A} = \begin{pmatrix} \cos\alpha & \sin\alpha \\ -\sin\alpha & \cos\alpha \end{pmatrix} \tag{28}$$

with $0 \leq \alpha < \pi/2$.

Let us consider the sum of the square SV of $\boldsymbol{H}_v\boldsymbol{A}\boldsymbol{\Sigma}$

$$\lambda_1^2 + \lambda_2^2 = \|\boldsymbol{H}_v\boldsymbol{A}\boldsymbol{\Sigma}\|_F^2 = trace\left(\boldsymbol{H}_v\boldsymbol{A}\boldsymbol{\Sigma}\boldsymbol{\Sigma}\boldsymbol{A}^*\boldsymbol{H}_v\right) \tag{29}$$

$$= p_0(\rho_1\sin^2\psi + \rho_2\cos^2\psi + (\rho_1 - \rho_2)\cos(2\psi)\cos^2\alpha). \tag{30}$$

As $\rho_1 > \rho_2$, for every λ_1 the maximum value of λ_2 is obtained for $\alpha = 0$, which means $\boldsymbol{A} = \boldsymbol{I}_2$.

APPENDIX II
PROOF OF (11)

The matrix $\boldsymbol{B}^*$ is unitary and the general form of a unitary matrix in dimension 2 is given by (24). The matrix $\boldsymbol{B}^*$ can be expressed as

$$\boldsymbol{B}^* = \begin{pmatrix} e^{j\alpha_1} & 0 \\ 0 & e^{j\alpha_2} \end{pmatrix} \begin{pmatrix} \cos\alpha & \sin\alpha\, e^{j(\alpha_3-\alpha_1)} \\ -\sin\alpha & \cos\alpha\, e^{j(\alpha_4-\alpha_2)} \end{pmatrix} = \boldsymbol{B}_1\boldsymbol{B}_2. \tag{31}$$

The difference vector distance is given by

$$\begin{aligned} d_{\breve{x}} &= \|\boldsymbol{H}_v\boldsymbol{\Sigma}\boldsymbol{B}^*\breve{\boldsymbol{x}}\| && (32)\\ &= \|\boldsymbol{H}_v\boldsymbol{\Sigma}\boldsymbol{B}_1\boldsymbol{B}_2\breve{\boldsymbol{x}}\| && (33)\\ &= \|\boldsymbol{B}_1\boldsymbol{H}_v\boldsymbol{\Sigma}\boldsymbol{B}_2\breve{\boldsymbol{x}}\| = \|\boldsymbol{H}_v\boldsymbol{\Sigma}\boldsymbol{B}_2\breve{\boldsymbol{x}}\|. && (34) \end{aligned}$$

The last equality is verified thanks to the unitarity and the diagonality of $\boldsymbol{B}_1$. Hence the matrix $\boldsymbol{B}_1$ has no influence on $d_{\breve{x}}$. Finally by using the initial unitarity constraint (25) on $\boldsymbol{B}^*$ and by setting $\varphi = (\alpha_3 - \alpha_1)$ we obtain (11).

APPENDIX III
SEARCH DOMAIN LIMITATION

Considering the symmetries in usual constellations (*e.g.*, centered square constellations) the difference vectors $\breve{\boldsymbol{x}} = [x_1, x_2]^T$ have the following properties

i. $(\breve{\boldsymbol{x}})^c = [x_1^*, x_2^*]^T$ is a difference vector.

ii. $(\breve{\boldsymbol{x}})^d = [x_1^*, -x_2^*]^T$ is a difference vector.

iii. $(\breve{\boldsymbol{x}})^e = [x_2, x_1]^T$ is a difference vector.

We can limit the search to $0 \leq \varphi \leq \pi$, because if we replace φ with $-\varphi$, the global channel $\boldsymbol{H}_g = \boldsymbol{H}_v\boldsymbol{F}_D$ becomes $(\boldsymbol{H}_g)^c$ (conjugate, non transposed matrix). We have

$$\|(\boldsymbol{H}_g)^c\ \breve{\boldsymbol{x}}\| = \|\boldsymbol{H}_g\ (\breve{\boldsymbol{x}})^c\|\,, \tag{35}$$

and using property (i), it is obvious that it is useless to test $-\varphi$ when φ was already tested.

We can even limit the search to $0 \leq \varphi \leq \pi/2$. If φ is replaced with $\pi - \varphi$, the matrix $\boldsymbol{B}_\varphi$ becomes

$$\boldsymbol{B}_{\pi-\varphi} = \begin{pmatrix} 1 & 0 \\ 0 & -e^{-i\varphi} \end{pmatrix}. \tag{36}$$

It can be written

$$(\boldsymbol{B}_{\pi-\varphi}\breve{\boldsymbol{x}})^c = \boldsymbol{B}_{\varphi}\,(\breve{\boldsymbol{x}})^d\,. \tag{37}$$

We have

$$\begin{aligned}\|\boldsymbol{H}_v\boldsymbol{\Sigma}\boldsymbol{B}_{\theta}\boldsymbol{B}_{\pi-\varphi}\breve{\boldsymbol{x}}\| &= \|(\boldsymbol{H}_v\boldsymbol{\Sigma}\boldsymbol{B}_{\theta}\boldsymbol{B}_{\pi-\varphi}\breve{\boldsymbol{x}})^c\| &(38)\\ &= \|\boldsymbol{H}_v\boldsymbol{\Sigma}\boldsymbol{B}_{\theta}\boldsymbol{B}_{\varphi}(\breve{\boldsymbol{x}})^d\| &(39)\end{aligned}$$

by using (37). From property (ii), it is obvious that it is useless to test $\pi-\varphi$ when φ was already tested.

Finally, as far as θ is concerned, the search domain can be limited to $0 \le \theta \le \pi/4$. If θ is replaced with $\pi/2-\theta$, the matrix $\boldsymbol{B}_{\theta}$ becomes

$$\boldsymbol{B}_{\pi/2-\theta} = \begin{pmatrix} \sin\theta & \cos\theta \\ -\cos\theta & \sin\theta \end{pmatrix}. \tag{40}$$

We have

$$\begin{aligned}\boldsymbol{B}_{\pi/2-\theta}\boldsymbol{B}_{\varphi}\breve{\boldsymbol{x}} &= \begin{pmatrix} (\cos\theta)\,e^{i\varphi}x_2 + (\sin\theta)\,x_1 \\ (\sin\theta)\,e^{i\varphi}x_2 - (\cos\theta)\,x_1 \end{pmatrix} = \begin{pmatrix} 1 & 0 \\ 0 & -1 \end{pmatrix}\begin{pmatrix} \cos\theta & \sin\theta \\ -\sin\theta & \cos\theta \end{pmatrix}\begin{pmatrix} e^{i\varphi}x_2 \\ x_1 \end{pmatrix}\\ &= e^{i\varphi}\begin{pmatrix} 1 & 0 \\ 0 & -1 \end{pmatrix}\boldsymbol{B}_{\theta}\begin{pmatrix} 1 & 0 \\ 0 & e^{-i\varphi} \end{pmatrix}\begin{pmatrix} x_2 \\ x_1 \end{pmatrix} = e^{i\varphi}\begin{pmatrix} 1 & 0 \\ 0 & -1 \end{pmatrix}\boldsymbol{B}_{\theta}\,(\boldsymbol{B}_{\varphi})^c\,(\breve{\boldsymbol{x}})^e\,. \end{aligned}\tag{41}$$

$e^{i\varphi}$ and the matrix whose diagonal is $[1,-1]$ have no influence on the distance. Furthermore it was proved that replacing $\boldsymbol{B}_{\varphi}$ with $(\boldsymbol{B}_{\varphi})^c$ (*i.e.*, replacing φ with $-\varphi$) does not act on the distance either. Finally, from property (iii), it is proved it is useless to test $\pi/2-\theta$ when θ was already tested.

APPENDIX IV
EXACT VALUE OF $\boldsymbol{F}_{r1}$ ANGLES

Fig. 13 plots the received constellation on the first virtual subchannel for $\psi = 0$ and two arbitrary angles θ and φ of the precoding matrix $\boldsymbol{F}_D$. The 16 points labeled from 'A' to 'P' correspond to the received symbol $z = \sqrt{\rho_1 p_0}(\cos\theta s_1 + \sin\theta e^{j\varphi}s_2)$ for $\boldsymbol{s} = [s_1\ s_2]^T \in \mathcal{S}$. Let us note z_A the affix (complex number representative) of the point 'A', and so on for the 16 points. The minimum distance $d_{\min}$ is optimized such that the nearest neighbors have the same distance. Thanks to symmetries exhibited in Fig. 13, the optimized solution can be obtained, for example, for[7] $d_{BE} = d_{BJ} = d_{EJ}$. The evaluation

[7] d_{XY} stands for the distance between points 'X' and 'Y' and is given by $d_{XY} = |z_X - z_Y|$.

of these distances is straightforward, we obtain

$$d_{BE}^2 = 2p_0\rho_1(1-\sin(2\theta)\cos\varphi) \quad (42)$$

$$d_{BJ}^2 = 2p_0\rho_1\sin^2\theta \quad (43)$$

$$d_{EJ}^2 = 2p_0\rho_1(1+\sin^2\theta-\cos(2\theta)(\cos\varphi+\sin\varphi)) \quad (44)$$

for $\theta \in [0, \pi/4]$ and $\varphi \in [0, \pi/2[$. Using (42) and (43) we obtain

$$\tan\theta = 1/(2\cos\varphi), \quad (45)$$

and using (42) and (44) we obtain

$$\tan\theta = 2\sin\varphi. \quad (46)$$

From (45) and (46) the optimal angle φ can be determined with $\sin 2\varphi = 1/2$ and we obtain $\varphi = \pi/12$. The optimal angle θ can be then determined with $\tan\theta = 1/(2\cos(\pi/12)) = (\sqrt{3}-1)/\sqrt{2}$. One should note that the optimized solution looks like a 16-QAM constellation rotated by an angle of 15^o.

REFERENCES

[1] G. D. Golden, G. J. Foschini, P. W. Wolnianski, and R. A. Valenzuela. V-BLAST: A high capacity space-time architecture for the rich-scattering wireless channel. In *Proc. of Int. Symp. on Advanced Radio Technologies*, Boulder, CO, Sept. 9-11 1998.

[2] G. J. Foschini and M. J. Gans. On limits of wireless communications in a fading environment when using multiple antennas. *Wireless Personal Communications*, 6(3):311–335, Mar. 1998.

[3] V. Tarokh, N. Seshadri, and A. R. Calderbank. Space-time codes for high data rate wireless communication: Performance criterion and code construction. *IEEE Trans. Inform. Theory*, 44:744–765, Mar. 1998.

[4] S. M. Alamouti. A simple diversity technique for wireless communications. *IEEE J. Sel. Areas Commun.*, 16(8):1451–1458, Oct. 1998.

[5] I. E. Telatar. Capacity of multi-antenna Gaussian channels. *Eur. Trans. Telecommun.*, 10(6):585–595, Nov./Dec. 1999.

[6] H. Sampath, P. Stoica, and A. J. Paulraj. Generalized linear precoder and decoder design for MIMO channels using the weighted MMSE criterion. *IEEE Trans. Commun.*, 49(12):2198–2206, Dec. 2001.

[7] A. Scaglione, P. Stoica, S. Barbarossa, G. B. Giannakis, and H. Sampath. Optimal designs for space-time linear precoders and decoders. *IEEE Trans. Signal Processing*, 50(5):1051–1064, May 2002.

[8] P. Rostaing, O. Berder, G. Burel, and L. Collin. Minimum BER diagonal precoder for MIMO digital transmissions. *Signal Processing*, 82(10):1477–1480, Oct. 2002.

[9] P. Stoica and G.A. Ganesan. Maximum-snr spatial-temporal formatting designs for mimo channels. *IEEE Trans. Signal Processing*, 50(12):3036–3042, Dec. 2002.

[10] X. Zhu and R. D. Murch. Performance analysis of maximum likelihood detection in a MIMO antenna system. *IEEE Trans. Commun.*, 50(2):187–191, Feb. 2002.

[11] J. Boutros, E. Viterbo, C. Rastello, and J. C. Belfiore. Good lattice constellations for both Rayleigh fading and Gaussian channels. *IEEE Trans. Inform. Theory*, 42:502–518, Mar. 1996.

[12] C. Lamy. *Communications à grande efficacité spectrale sur le canal à évanouissements*. Phd thesis in electrical and computer engineering, ENST Paris, France, Apr. 2000.

[13] R. W. Heath Jr. and A. Paulraj. Switching between multiplexing and diversity based on constellation distance. In *Proc. of 38th Annual Allerton Conf. on Commun., Control and Computing*, Monticello, Illinois, USA, Oct. 4-6 2000.

[14] R. W. Heath and A. Paulraj. Antenna selection for spatial multiplexing systems based on minimum error rate. In *Proc. of IEEE Int. Conf. Commun. (ICC) 2001*, Helsinki, Finland, June 11-14 2001.

[15] L. Collin, O. Berder, P. Rostaing, and G. Burel. Soft vs. hard antenna selection based on the minimum distance for MIMO systems. In *Proc. Asilomar Conf. on Signals, Systems and Computers*, Pacific Grove, CA, USA, Nov. 3-7 2002.

[16] K. J. Kerpez. Constellations for good diversity performance. *IEEE Trans. Commun.*, 41(9):1412–1421, Sept. 1993.

[17] C. Lamy and J. Boutros. On random rotations diversity and minimum MSE decoding of latices. *IEEE Trans. Inform. Theory*, 46(4):1584–1589, July 2000.

[18] R. Van Nee, A. Van Zelst, and G. Awater. Maximum likelihood decoding in a space division multiplexing system. In *IEEE Fall Veh. Technol. Conf. (VTC)*, pages 6–10, Sept. 2000.

[19] P. Stoica and G. Ganesan. Maximum-SNR spatial-temporal formatting designs for MIMO channels. *IEEE Trans. Signal Processing*, 50(12), Dec. 2002.

[20] G. D. Golden, C. J. Foschini, R. A. Valenzuela, and P. W. Wolniansky. Detection algorithm and initial laboratory results using V-BLAST space-time communication architecture. *Elec. Letters*, 35(1):14–15, Jan. 1999.

[21] V. Tarokh, A. Naguib, N. Seshadri, and A.R. Calderbank. Space-time code for high data rate wireless communication: Performance criteria in the presence of channel estimation errors, mobility, and multiple paths. *IEEE Trans. Commun.*, 47(2), Feb. 1999.

step	i	method	$\boldsymbol{F}_i$	$\boldsymbol{G}_i$	$\boldsymbol{H}_{v_i}$	$\boldsymbol{R}_{v_i}$
noise whitening	1	EVD: $\boldsymbol{R} = \boldsymbol{Q}_1 \boldsymbol{\Lambda}_1 \boldsymbol{Q}_1^*$	$\boldsymbol{F}_1 = \boldsymbol{I}_{n_T}$	$\boldsymbol{G}_1 = \boldsymbol{\Lambda}_1^{-\frac{1}{2}} \boldsymbol{Q}_1^*$	$\boldsymbol{H}_{v1} = \boldsymbol{G}_1 \boldsymbol{H} \boldsymbol{F}_1$	$\boldsymbol{R}_{v1} = \boldsymbol{G}_1 \boldsymbol{R} \boldsymbol{G}_1^* = \boldsymbol{I}_{n_R}$
channel diagonalization	2	SVD: $\boldsymbol{H}_{v1} = \boldsymbol{A}_2 \boldsymbol{\Sigma}_2 \boldsymbol{B}_2^*$	$\boldsymbol{F}_2 = \boldsymbol{B}_2$	$\boldsymbol{G}_2 = \boldsymbol{A}_2^*$	$\boldsymbol{H}_{v2} = \boldsymbol{\Sigma}_2$	$\boldsymbol{R}_{v2} = \boldsymbol{I}_{n_R}$
dimensionality reduction	3	$\boldsymbol{\Sigma}_2 = \begin{pmatrix} \boldsymbol{\Sigma}_r & 0 \\ 0 & 0 \end{pmatrix}$	$\boldsymbol{F}_3 = \begin{pmatrix} \boldsymbol{I}_b \\ 0 \end{pmatrix}$	$\boldsymbol{G}_3 = \begin{pmatrix} \boldsymbol{I}_b & 0 \end{pmatrix}$	$\boldsymbol{H}_{v3} = \boldsymbol{G}_3 \boldsymbol{H}_{v2} \boldsymbol{F}_3 = \boldsymbol{H}_v$	$\boldsymbol{R}_{v3} = \boldsymbol{R}_v = \boldsymbol{I}_b$

TABLE I

STEPS TO OBTAIN THE DIAGONAL MIMO SYSTEM IN CASE OF CSI AT THE TRANSMITTER.

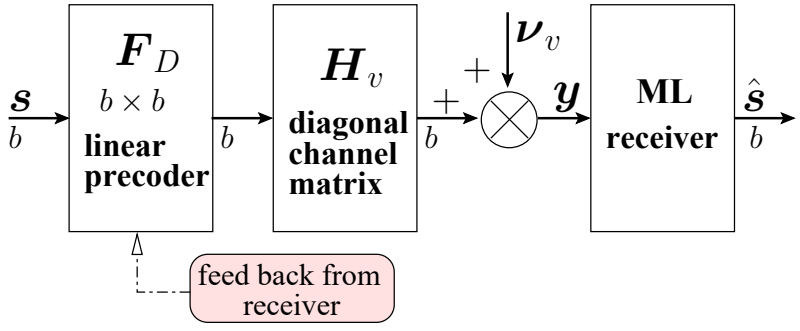

Fig. 1. MIMO equivalent transmission system with a linear precoder in case of CSI.

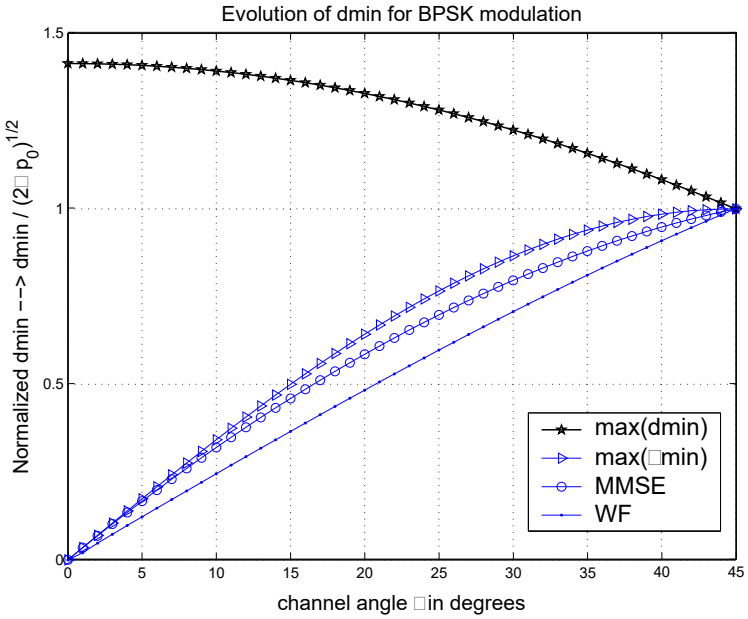

Fig. 2. Normalized Euclidean distance $d_{\min}/\sqrt{2\rho p_0}$ for BPSK modulation.

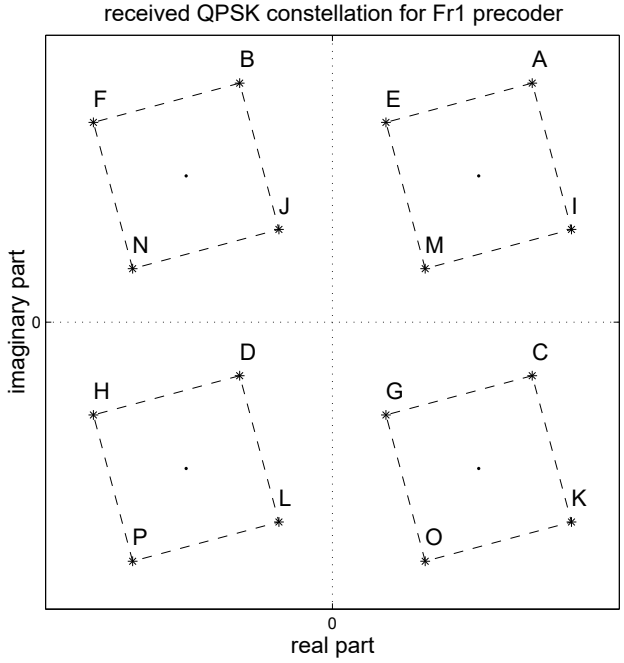

Fig. 3. Received constellation for the precoder $\boldsymbol{F}_{r1}$.

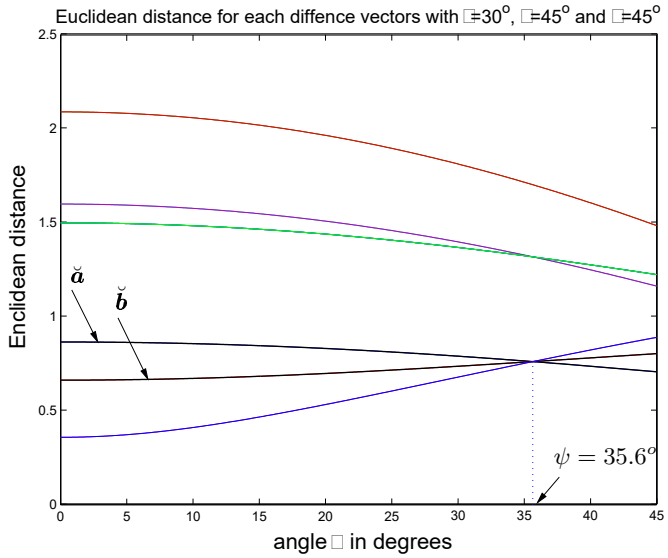

Fig. 4. Euclidean distance with $\varphi = 45^o$ and $\theta = 45^o$ for each difference vector with respect to ψ (in degrees). The channel angle is $\gamma = 30^o$.

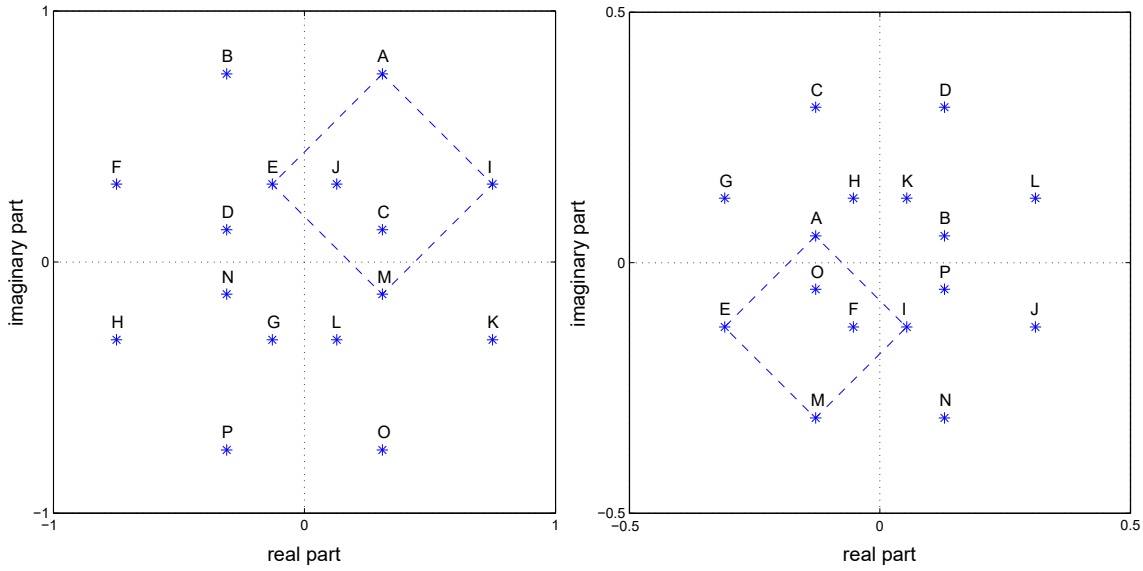

(a) first virtual subchannel (b) second virtual subchannel

Fig. 5. Received constellations for the precoder $\boldsymbol{F}_{octa}$.

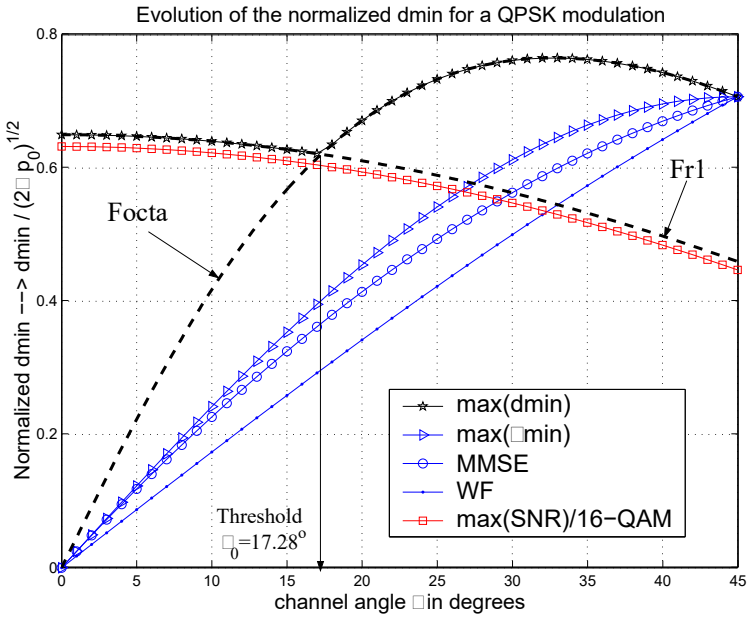

Fig. 6. Normalized Euclidean distance $d_{\min}/\sqrt{2\rho p_0}$ for QPSK modulation.

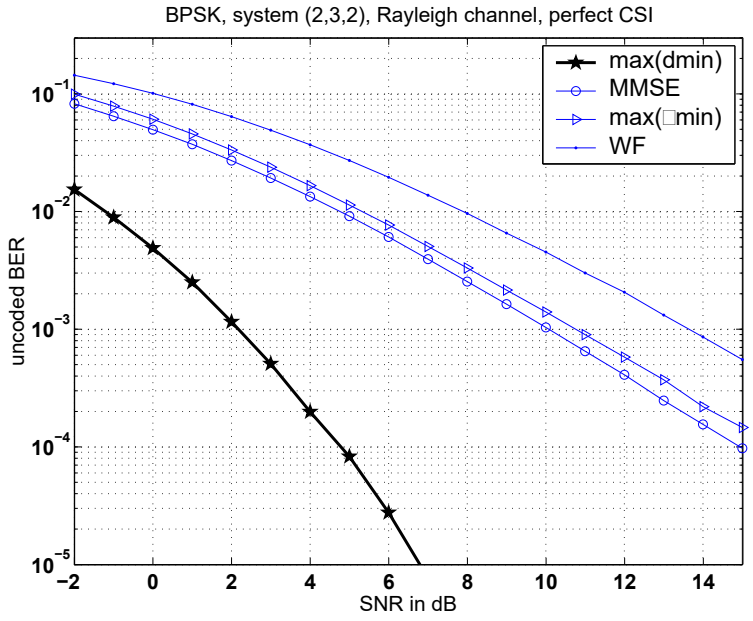

Fig. 7. Uncoded BERs for BPSK modulation.

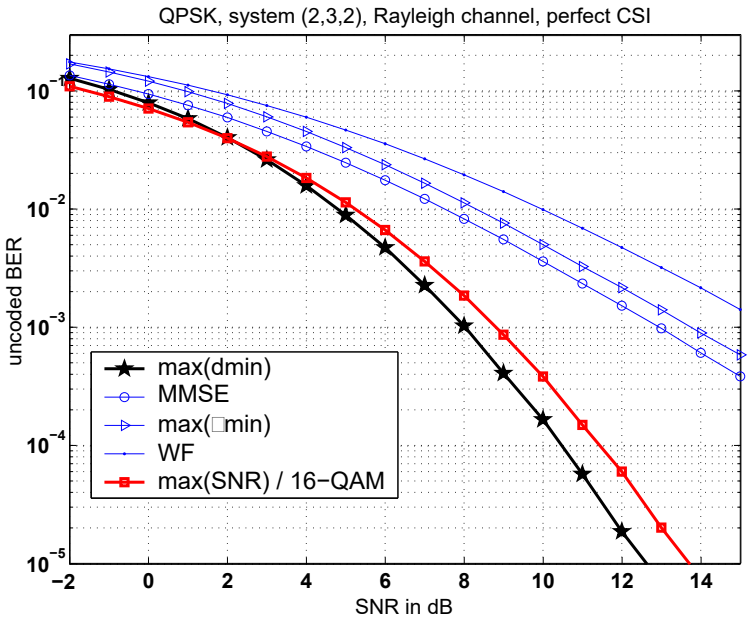

Fig. 8. Uncoded BERs for QPSK modulation.

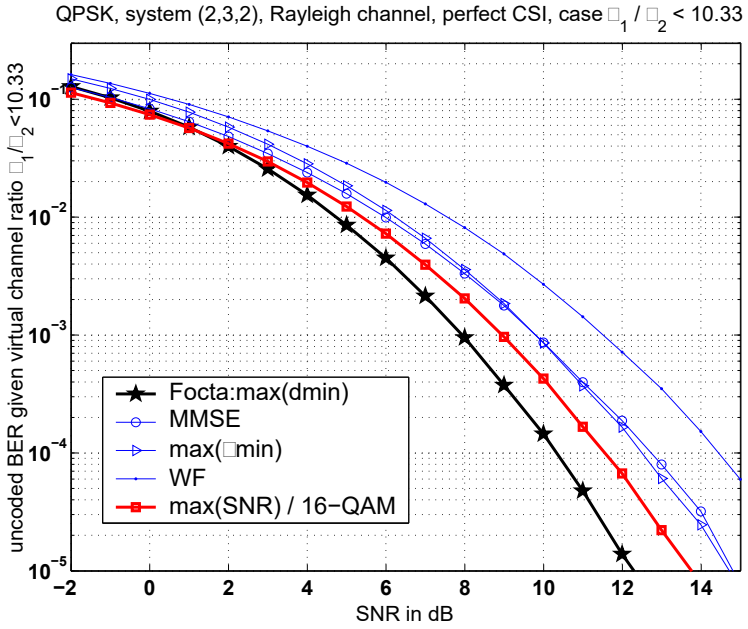

Fig. 9. Uncoded BERs for QPSK modulation assuming the precoding scheme $\boldsymbol{F}_{octa}$ (case $\frac{\rho_1}{\rho_2} < 10.33$).

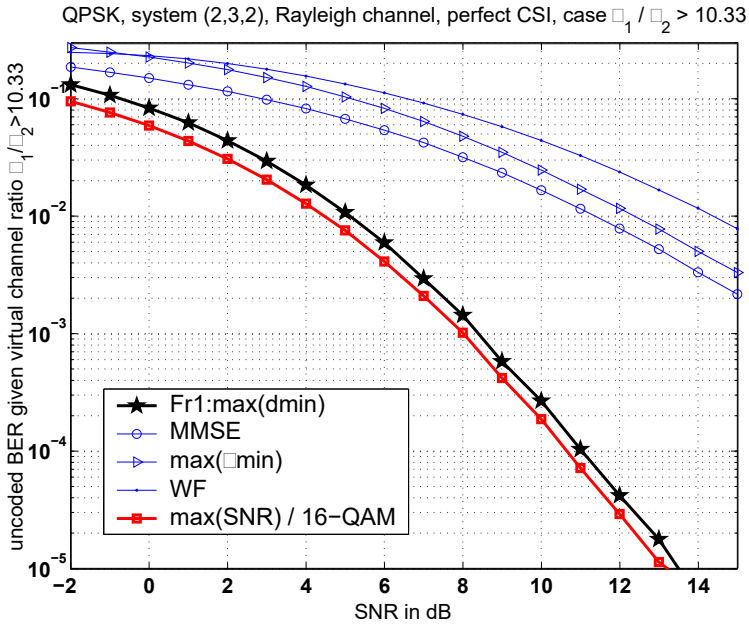

Fig. 10. Uncoded BERs for QPSK modulation assuming the precoding scheme $\boldsymbol{F}_{r1}$ (case $\frac{\rho_1}{\rho_2} > 10.33$).

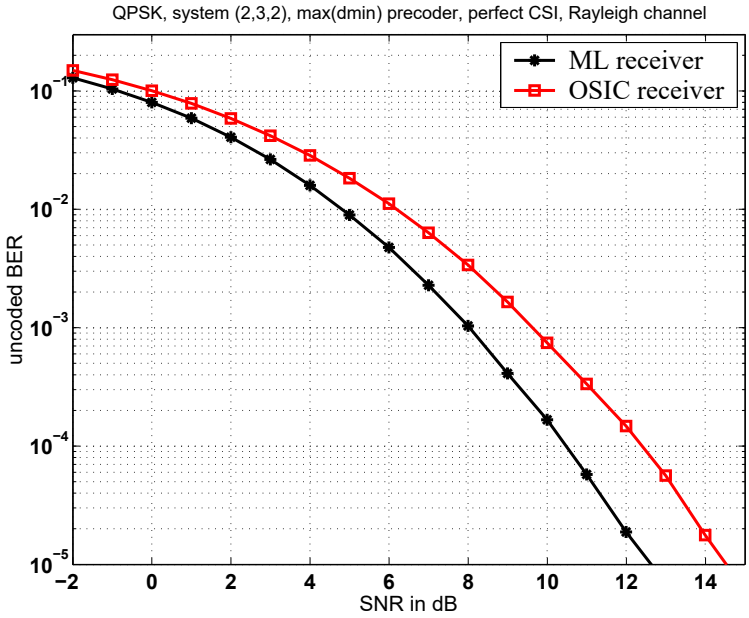

Fig. 11. Uncoded BERs for the $\max(d_{\min})$-QPSK design using the ML and the OSIC receivers.

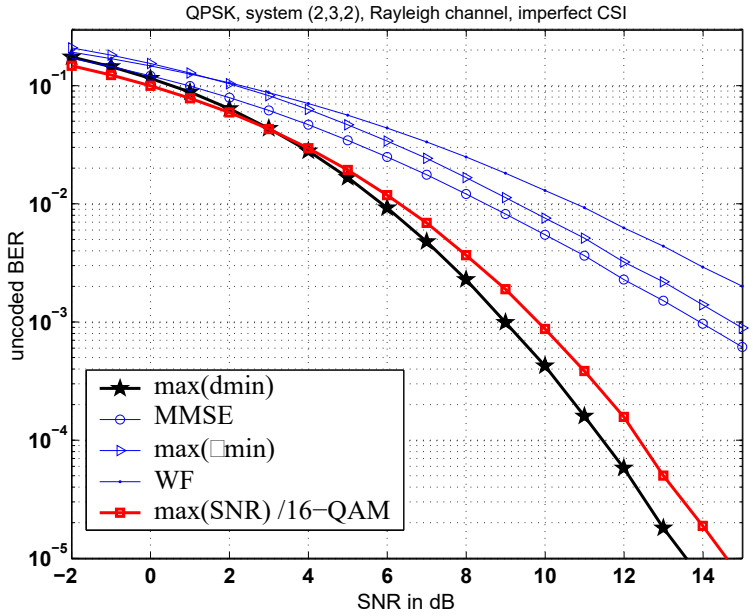

Fig. 12. Uncoded BERs for QPSK modulation in case of imperfect CSI.

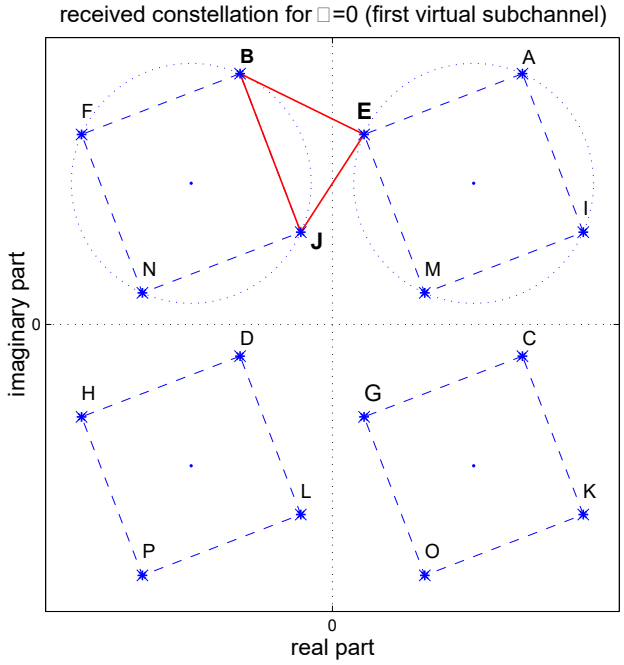

Fig. 13. Non-optimized received constellation on the first virtual subchannel for $\psi = 0$ (QPSK modulation).